Applied Robust Control for Vibration Suppression in Parallel Robots

Stephan Algermissen, Ralf Keimer, Michael Rose, and Elmar Breitbach

***Abstract*— Automation within the range of handling and assembly applications requires qualified solutions due to the complex technological processes. The long-term goals are the reduction of cycle time and an increase of the process quality. They can be achieved by innovative concepts which are based on parallel kinematics, realizing higher speeds and accelerations with constant accuracy compared to conventional serial robot structures. High accelerations are equivalent to high forces in the starting and deceleration phase of the trajectory. The vibrations of the robot structure induced thereby and the following decaying procedure are unwanted and time-consuming in handling and assembly applications, in particular during accurate placement of components. In the context of German DFG Collaborative Research Center 562 'Robotic Systems for Handling and Assembly' a parallel robot with two degrees of freedom, made of CFRP components, was built-up at the Institute of Composite Structures and Adaptive Systems, DLR, Germany. The specialty of this robot is the integrated vibration suppression introduced by active rods, that are driven by piezoceramic stacks. These active rods are addressed by a robust controller, which generates the suitable control variable using measurements of the oscillations of the effector. The robot is not a time-invariant system and therefore its vibration characteristics changes depending on the position, the loading condition and the way the robot was assembled. These facts make high demands on the robust controller, which must output suitable signals to the actuators for the suppression of vibrations in each condition, without becoming unstable.**

In this article the parallel robot and its components are presented. A special focus is put on the design of the robust controller for vibration suppression. Furthermore, the strategies used for the employment of the control in the entire work space of the robot are shown. A further topic is the system identification of the plant, which must be accomplished fast and reliably with a variant system like this. Finally the effectiveness of the concepts and procedures presented here is shown with experimental data.

***Index Terms*— Adaptive Systems, Adaptronic, Parallel Robot, Robust Control, Robust-Gain-Scheduling, Smart Structures**

I. Introduction

THE industrial robot is the central element of a flexible aligned assembly. The innovation potential of classical, serial robots for handling and assembly is nearly exhausted [1]. The use of more efficient drives in combination with links of higher stiffness increases the moved robot mass, which requires again an increase of the drive power. Therefore, conventional robot systems cannot satisfy the demands on further increase of speed and accuracy any longer. Thus,

All authors are with the Institute of Composite Structures and Adaptive Systems, DLR e.V. (German Aerospace Center), Lilienthalplatz 7, Braunschweig, Germany.

Further Author Information: Send Correspondence to Stephan Algermissen E-mail: Stephan.Algermissen@dlr.de, Telephone: +49 531 295 2347

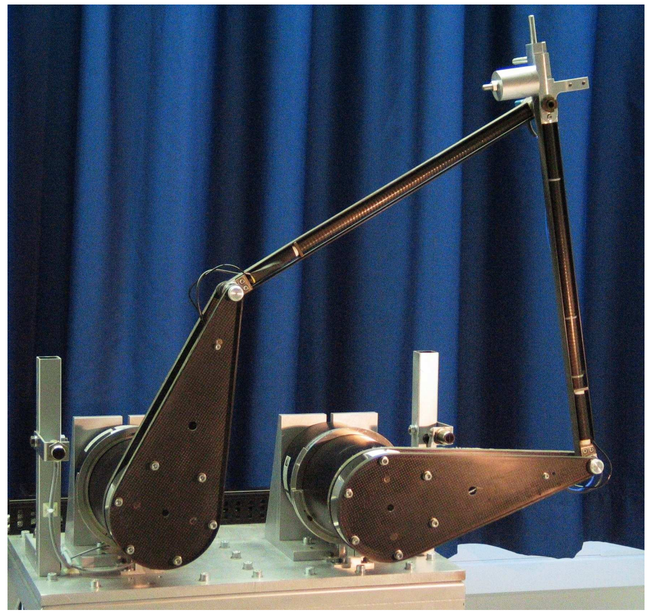

Fig. 1. Test Platform Parallel Robot FIVE-BAR

an improvement of the productivity has to be obtained by new robot systems. Parallel structures represent a promising alternative. They have a small ratio between moved robot mass and payload. The vibrations of such light structures which inevitably arise with high accelerations, have a reduction of the process quality as consequence. For avoidance of unwanted oscillations the field of adaptive systems is a key technology. Adaptive systems use structure-integrated actuators and sensors for the control of vibrations of the whole structure. Especially during the so-called Pick-and-Place operations, in which components are placed fast and accurate, smart systems are an ideal technology for reduction of decaying procedures of the structure.

In order to extend the application area of parallel robots, fundamental investigations regarding new structural concepts, adapted mechanical components and adaptive systems are carried out together with TU Braunschweig in the context of the Collaborative Research Center (SFB) 562: 'Robot Systems for Handling and Assembly'. Within the range of adaptive systems for parallel robots, specific active components, models for describing the vibration behavior of the structure and new approaches for structural control are developed. This article presents the results which were worked out within the Collaborative Research Center 562 in the field of adaptive systems.

Fig. 2. CFRP Panel

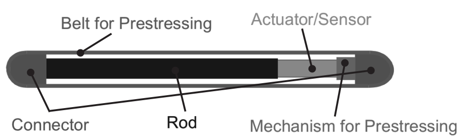

Fig. 3. Principle Active Rod

II. Configuration

The present test platform for adaptive systems in the SFB is FIVE-BAR, a planar parallel robot (2 DOF), s. Fig. 1. The specialty of this robot is the integration of adaptive components from the beginning of the design phase. This way the efficient integration of the components was possible.

The FIVE-BAR consists of two cranks and two active rods. The cranks consist of two CFRP panels each, s. Fig. 2, which are connected with a cylinder and a spacer made of aluminium. The core components of the structure are the active rods, s. Fig. 3, which are built up of a piezo stack and a unidirectional CFRP rod and linked up on pressure over a belt. The preloading is needed, since the piezo stacks can only be operated in the compressive stress domain. Additionally, a ceramic layer of the stack was electrically separated from the others in order to serve as a sensor layer for the measurement of internal forces. The actuator operates at a voltage of 0 to 1000 V.

The structure is driven by two direct drives. The effector for the attachment of the tool fitting is at the joint between the two active rods. At the effector a three-axis acceleration sensor is positioned for measuring the oscillations of the structure.

The control architecture is a proprietary development of the SFB [2]. An overview is given in Fig. 4. The interaction with sensors and actuators over A/D and D/A converters is realized by task specific nodes. A node consists of a DSP board with TI C6711 processor, an I/O board and a Firewire board. The FIVE-BAR has two such nodes, one for the direct-drive control and one for the structural control. The nodes are connected with the control computer over the Firewire bus. On the control computer the realtime processing system QNX is used [4]. The middleware MIRPA-X, developed in the SFB, provides

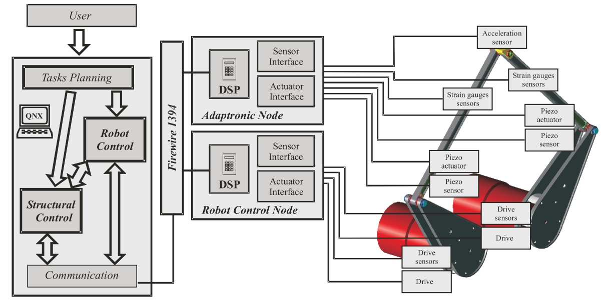

Fig. 4. Control Architecture of FIVE-BAR [3]

the correct processing of all realtime tasks, makes message channels available and administers shared memory regions. Within the tasks called by MIRPA-X once in the control cycle the controller computation takes place. The systemcycle is given by the Firewire clock and amounts to presently 2.67 kHz. Within each cycle data are read from the bus, processed by the realtime tasks and sent back as control variables over the bus to the nodes.

III. Control

A. Objectives and Strategy

The goal of the adaptive systems is the reduction of unwanted vibrations of the structure. For this high-dynamic parallel robot for handling and assembly, the performance criterion is the fast and accurate placement of components in Pick-and-Place operations. In order to fulfill this criterion at trajectories with high brake acceleration, the structural control must shorten the duration of the decaying process of the effector significantly.

Tests with FIVE-BAR showed that the mode shapes, which are excited by disturbances, are mainly formed perpendicular to the working plane of the robot (z-direction). This has the consequence that the disturbances shift the effector almost exclusively in z-direction and move it out of the desired position. With the acceleration sensor, already mentioned above, it is possible to measure the influence of the disturbances directly at the effector. Therefore, the acceleration in z-direction was selected as controlled variable y. Measurements showed that after position-controlled moves with $4\,\mathrm{m/s}$ lateral accelerations of up to $3\,\mathrm{m/s^2}$ arise.

The actuators to be controlled are the piezo stacks, incorporated into the active rods. The stacks generate a longitudinal expansion of the rods, up to $70\,\mu\mathrm{m}$ in the unloaded case (free stroke) [5]. A set-up of the rods in one plane would have the consequence that oscillations out of the plane would not be controllable by longitudinal expansions of the rods. Therefore, the location of the rods is shifted in z-direction by $30\,\mathrm{mm}$. The piezo stacks are driven by a high voltage amplifier around a mean voltage of $500\,\mathrm{V}$. The input signal to the amplifier is amplified by the factor 200. The inputs of the two amplifiers are at the same time the control variables u_1 and u_2 of the control loop.

The robot structure is a time-variant system with respect to its vibration behavior. Different influences like the position

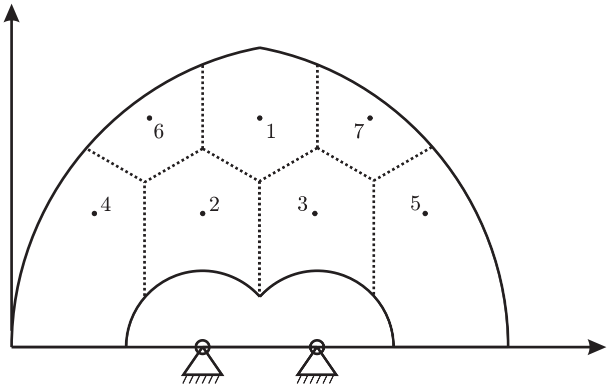

Fig. 5. Used Workspace of FIVE-BAR with Regions and Working Points

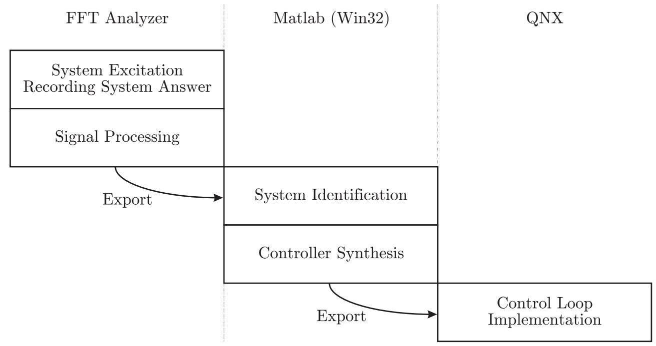

Fig. 6. Former Control Synthesis Process

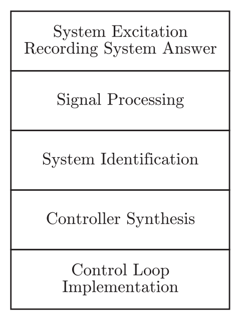

Fig. 7. New Control Synthesis Process

within the workspace and the mass at the effector lead to changes of the dynamic behavior during the runtime of the robot. These boundary conditions have crucial influence on the requirements to the structural control. Therefore the control must

- have good performance,
- stabilize the control system,
- be robust against position changes of the effector,
- be robust against mass changes of the structure

in the entire workspace. In order to reduce these high requirements and increase the performance, a certain foreknowledge can already be used in the synthesis of the controller. The position of the effector in the workspace is known by means of the position control of the direct-drives. Instead of a controller design for the entire workspace, an ideal controller for each position can be synthesized with the help of this knowledge, at least theoretically. The position is the only value, which can be evaluated in this kind, since no information about the mass configuration is present at runtime. For purely practical reasons the workspace is divided into a small, finite number of regions. Each region contains an operating point in which a controller is designed. With FIVE-BAR there are seven regions at present, s. Fig. 5. The operating points are distributed in regular distances over the workspace. The controller selected depends on the endpoint of the trajectory. The operating point closest to the endpoint decides about which controller is selected. For this reason each region has the shape of a Voronoi-polygon. In order to be able to formulate demands on the robustness of the control system during the synthesis process, $\mathcal{H}_\infty$ controllers are used exclusively. The method used here is called Robust-Gain-Scheduling.

A large problem, which emerges again and again in adaptive systems, is the sensitivity of the vibration behavior of a structure in relation to structural changes and the necessary redesign of the controller. As an example of changes to FIVE-BAR the disassembly of the CFRP structure from the direct-drives for maintenance purposes or tests can be mentioned. After such an disassembly and assembly cycle the vibration behavior of the structure changed, so that eigenfrequencies shifted or changed their amplitudes and even new ones arose. Therefore it cannot be guaranteed that controllers, designed before, are still stable and possess sufficient performance. For safety reasons a new synthesis is inevitable. In this article a procedure is presented that enables a fast redesign of the controllers on the target system (QNX).

The design of a controller is carried out with a plant that was identified by measurements. With the help of the two actuators the structure was excited to oscillations, which were sensed with the acceleration sensor. In this way two frequency responses (FRF) were measured between the actuator voltages u_1 and u_2 and the acceleration of the effector in z-direction y. They were described by means of a system identification by a state-space model [6], [7]. In practice the analytic formulation of the plant proved to be less practicable, since a controller design on this basis presupposes an exact knowledge of the models parameters. To determine the models parameters measurements must be done likewise. Besides, their identification becomes more difficult.

The former procedure of control synthesis process is represented in Fig. 6. The measurement and the computation of the FRF were carried out with a FFT Analyzer. Export and import filters enabled further processing of the data on a Windows PC using Matlab. With the help of a system identification toolbox the FRF could be identified in form of a state-space model. Based on this model, the controller was designed with another toolbox. Export routines transformed the designed controller into C source code, which has been transferred afterwards to the actual QNX control computer. Due to the use of three different systems, FFT Analyzer, Windows PC and QNX, and the export and import procedures this method is time consuming. The problem of the sensitivity, mentioned above, can only be solved conditionally. After any disassembly and assembly of the structure all devices must be on site and the entire synthesis procedure must be repeated.

The procedure could substantially be simplified by the implementation of all modules on the QNX computer, s. Fig. 7. Porting important modules such as system identification and controller synthesis, former only possible under Matlab, to C source code, succeeded by the help of the Subroutine Library in System and Control Theory (SLICOT) [8], [9] from the NICONET Society. With the centralization of the entire controller development chain on the QNX computer, it is now possible to shorten the development time drastically in relation to the old procedure. Reaction to short term changes of the structure and to the problem of sensitivity can be carried out faster in this way. Furthermore the two other systems, FFT Analyzer and Windows PC, will be redundant and do not have to be present anymore. In the following sections the development chain is presented and the application of the SLICOT routines is explained.

B. Realization

On the QNX control computer the control of the structure is implemented as a process with two threads, the MainThread and the RealtimeThread. The RealtimeThread, explained earlier, is called in the system cycle by 2.67 kHz by MIRPA-X. It is implemented as finite state machine, which controls the system or records data for the system identification, depending upon the mode of operation. The eigenfrequencies which should be controlled lie in the range from 0 to 100 Hz, therefore the control of the structure runs only with 222.22 Hz. This frequency scaling by the factor 12 is done in the RealtimeThread. The anti-aliasing filters on the structural control node were adjusted due to the control cycle to a cut-off frequency of 100 Hz. The MainThread makes a command line menu for settings of the control process available. Over this menu the entire controller development is operated.

The use of SLICOT under QNX has the difficulty that all SLICOT routines are implemented in FORTRAN77, but no compiler under QNX is available. The LAPACK and BLAS routines needed by SLICOT are written in FORTRAN77 likewise, but a translation for C exists [10]. Only remedy is the use of the FORTRAN to C converter `f2c` [11]. In this way the most important routines for this project could be translated into C and made usable under QNX.

C. Signal Processing

For the identification of the plant the structure is excited with the actuators and the system answer is measured by the three-axis acceleration sensor at the effector. In the present development status only a single-input-single-output (SISO) system can be identified, therefore actuator 1 (u_1) is selected as plant input. The excitation signal must excite the entire spectrum which has to be identified. In practice the excitation with a sweep sine from 0 to 100 Hz worked satisfactorily. To improve the quality of the signal, the acceleration of the effector in z-direction (y) is recorded with 2.67 kHz system cycle. Speeding the system identification up, the recorded signal is sampled down by means of own routines to the control cycle of 222.22 Hz. The number of samples with this cycle should be 4096, which would have a sweep time from app. 18.4 s as consequence. Therefore the number of samples which have to be recorded is 12·4096=49152.

For the avoidance of aliasing effects the signal is filtered with a zero phase filter before sampling it down. This filter consists of two filter procedures with a Butterworth filter of fourth order with a cut-off frequency of 111.1 Hz. The first procedure is a usual filtering of a time signal [12]. For the second procedure the data filtered before are flipped in its temporal order and filtered again. The result is a filtered time signal which amplitude is reduced toward the cut-off frequency, but which phase remains unchanged. This way in- and output signals are sampled down.

D. System Identification

For system identification the measured signals u_1 and y are available in the time domain. Since a controller is installed in each operating point p, an identification must be done in each one also. An identification consists of the call of two SLICOT routines. The routine `IB01AD` composes a block Hankel matrix of the measured signals, executes a QR decomposition for these and returns the upper triangular factor R. The second routine, `IB01BD`, uses this matrix and computes the state-space model of the system by subspace identification methods [13]. The two routines have been enclosed in an own C function, which requires the data and the order of the system as parameters. The identified system must run through a stability test, since a stable solution for all orders does not exist.

In practice it was shown, that a good correlation of the identified system and the measured data can be obtained, if the identification is done with a higher order than required. Therefore the identification of FIVE-BAR starts at order 28 and checks the stability of the system found. If it is unstable, then the order is decreased by two and the identification is repeated. If even for the minimum order of 14 no stable system can be found, then the algorithm terminates and it should be measured again. The minimum order of 14 is an empirical value for FIVE-BAR, which can deviate with other structures. If the identification was already successful before reaching minimum order, then afterwards a reduction of the system to minimum order follows. The reduction is done with the SLICOT function `AB09MD` which uses a Balance & Truncate algorithm [14]. The result of the system identification is a discrete SISO state-space model

$$\underline{\underline{G}}_p = \left[\begin{array}{c|c} \underline{\underline{A}}_{g,p} & \underline{\underline{B}}_{g,p} \\ \hline \underline{\underline{C}}_{g,p} & \underline{\underline{D}}_{g,p} \end{array}\right] \quad (1)$$

with 14 states and a cycle time of 222.22 Hz for each operating point p.

E. Control Synthesis

Control loops of adaptive systems like FIVE-BAR, are mostly disturbance rejections. Their goal is the reduction of the influence of the disturbances on the controlled variable. In case of FIVE-BAR the unwanted vibrations are caused by

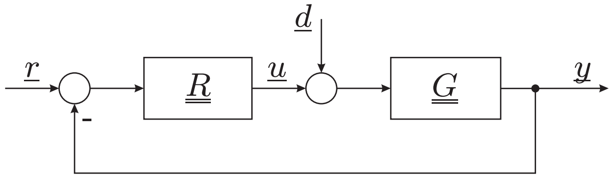

Fig. 8. Closed Control Loop

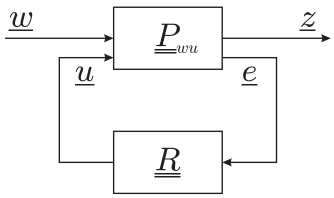

Fig. 9. Robust Controller Framework

acceleration procedures of the robot, like the deceleration at the end of a trajectory. Regarding the control loop in Fig. 8, it is apparent that the magnitude of the transfer function $\underline{\underline{S}}\,\underline{\underline{G}}$ from the disturbance $\underline{d}$ to the controlled variable $\underline{y}$ must be as small as possible, in order to obtain a good disturbance rejection. For the mathematical formulation of this requirement the $\mathcal{H}_\infty$ norm is very suitable, since it is equal to the maximum peak of the curve of the largest singular value of a transfer function. The $\mathcal{H}_\infty$ controller is based on the minimization of this norm [15]. In the general Robust Controller Framework in Fig. 9 it is the task of the $\mathcal{H}_\infty$ controller to tune the $\mathcal{H}_\infty$ norm of the transfer function $\underline{\underline{T}}_{zw}$ from the input $\underline{w}$ to the output $\underline{z}$ to less or equal one:

$$||\underline{\underline{T}}_{zw}||_\infty \leq 1 \tag{2}$$

To formulate the control objectives for this framework, one avails weighting functions $\underline{\underline{W}}_t$ and $\underline{\underline{W}}_{sg}$ and completes the control loop to the weighting scheme in Fig. 10. In order to ensure the robustness of the control loop in relation to modeling errors in form of multiplicative uncertainties at the output of $\underline{\underline{G}}$, one includes beside $\underline{\underline{S}}\,\underline{\underline{G}}$ also $\underline{\underline{T}}$ into the control synthesis. The transfer function $\underline{\underline{T}}_{zw}$ is now:

$$\underline{\underline{T}}_{zw} = \left[\underline{\underline{T}}\,\underline{\underline{W}}_t \;\; \underline{\underline{S}}\,\underline{\underline{G}}\,\underline{\underline{W}}_{sg}\right] \tag{3}$$

Where

$$\underline{\underline{S}} = \left[\underline{\underline{E}} + \underline{\underline{G}}\,\underline{\underline{R}}\right]^{-1} \tag{4}$$

is the sensitivity of the system and

$$\underline{\underline{T}} = \underline{\underline{G}}\,\underline{\underline{R}}\,\underline{\underline{S}} \tag{5}$$

the transfer function from $\underline{r}$ to $\underline{y}$.

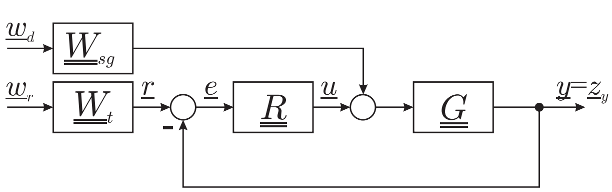

Fig. 10. Weighting Scheme

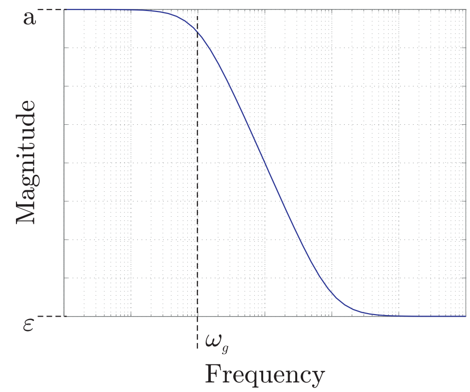

Fig. 11. FRF Magnitude of First Order Lowpass W^{-1}

A frequently used method for the constraint of the control variable $\underline{u}$ is the inclusion of the transfer function $\underline{\underline{R}}\,\underline{\underline{S}}$ into the controller synthesis. If one regards (5), then $\underline{\underline{T}}$ already contains the term $\underline{\underline{R}}\,\underline{\underline{S}}$. The plant $\underline{\underline{G}}$ is to be regarded as a further weighting of this value. Their influence on the control variable should be examined depending on the control system. A drastic reduction of the magnitude of $\underline{\underline{R}}\,\underline{\underline{S}}$ outside of the bandwidth of the controller is important, in order to avoid the excitation of higher harmonics, the so-called spillover effect.

The inverse of the weighting functions describe the desired singular value function of the weighted transfer functions. The inverse weighting functions $\underline{\underline{W}}_{sg}^{-1}$ and $\underline{\underline{W}}_t^{-1}$ are diagonal matrices with low-passes of first order with the continuous description

$$W^{-1} = \frac{\varepsilon s + a\omega_g}{s + \omega_g} \tag{6}$$

as diagonal elements. The function (6) has the pleasant characteristic that the upper and lower bound a and ε and the cut-off frequency ω_g can be found directly in the formal representation, s. Fig. 11. The design of the controller takes place in the z-domain, so that the weighting functions W must be discretised before. First of all W has been transformed into state-space representation [16].

$$W = \left[\begin{array}{c|c} -a\omega_g/\varepsilon & 1 \\ \hline \omega_g/\varepsilon\,(1 - a/\varepsilon) & 1/\varepsilon \end{array}\right] \tag{7}$$

With the help of the Tustin transformation, which represents a bilinear transformation, the system (7) is discretised at sampling time T.

$$W = \left[\begin{array}{c|c} \frac{2\varepsilon - a\omega_g T}{2\varepsilon + a\omega_g T} & \frac{2\varepsilon}{2\varepsilon + a\omega_g T} \\ \hline \frac{2\omega_g T(\varepsilon - a)}{\varepsilon(2\varepsilon + a\omega_g T)} & \frac{\omega_g T + 2}{2\varepsilon + a\omega_g T} \end{array}\right] \tag{8}$$

In the case of FIVE-BAR only a SISO system is controlled and thus (8) with the appropriate parameters corresponds directly to the weighting functions $\underline{\underline{W}}_{sg}$ and $\underline{\underline{W}}_t$. Their state-space representation for all operating points p reads

$$\underline{\underline{W}}_{sg,p} = \left[\begin{array}{c|c} \underline{\underline{A}}_{s,p} & \underline{\underline{B}}_{s,p} \\ \hline \underline{\underline{C}}_{s,p} & \underline{\underline{D}}_{s,p} \end{array}\right] \tag{9}$$

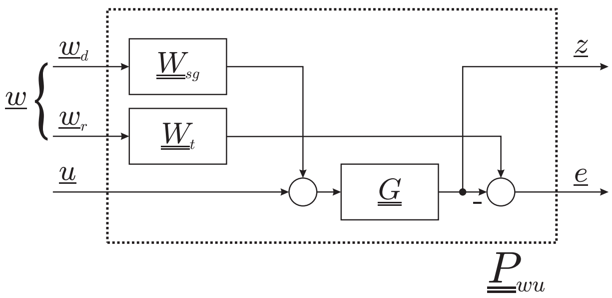

Fig. 12. Transformed Weighting Scheme without Controller

TABLE I
DIMENSIONS OF SYSTEMS

	States	Outputs	Inputs
$\underline{\underline{G}}_p$	n_{ng}	n_y	n_u
$\underline{\underline{W}}_{sg,p}$	n_{ns}	n_u	n_u
$\underline{\underline{W}}_{t,p}$	n_{nt}	n_y	n_y
$\underline{\underline{P}}_{wu,p}$	$n_{ng}+n_{ns}+n_{nt}$	$2n_y$	$2n_u+n_y$

and

$$\underline{\underline{W}}_{t,p} = \left[\begin{array}{c|c} \underline{\underline{A}}_{t,p} & \underline{\underline{B}}_{t,p} \\ \hline \underline{\underline{C}}_{t,p} & \underline{\underline{D}}_{t,p} \end{array}\right]. \tag{10}$$

The composition of the Robust Controller Framework, s. Fig. 9, is carried out by removing the controller $\underline{\underline{R}}$ from the weighting scheme in Fig. 10 and relocate the scheme. The new scheme in Fig. 12 matches the block $\underline{\underline{P}}_{wu}$ in the Robust Controller Framework, which is built up in the following. From Fig. 12 two equations for the outputs $\underline{z}$ and $\underline{e}$ can be derived.

$$\underline{z} = \underline{\underline{G}}\left(\underline{\underline{W}}_{sg}\underline{w}_d + \underline{u}\right) \tag{11}$$
$$\underline{e} = \underline{\underline{W}}_t\underline{w}_r - \underline{z} \tag{12}$$

By additive and multiplicative combinations of the state-space models $\underline{\underline{G}}$, $\underline{\underline{W}}_{sg}$ and $\underline{\underline{W}}_t$ from (1), (9) and (10) the system $\underline{\underline{P}}_{wu}$ is set together.

$$\underline{\underline{P}}_{wu} = \left[\begin{array}{ccc|ccc} \underline{\underline{A}}_t & 0 & 0 & \underline{\underline{B}}_t & 0 & 0 \\ 0 & \underline{\underline{A}}_s & 0 & 0 & \underline{\underline{B}}_s & 0 \\ 0 & \underline{\underline{B}}_g\underline{\underline{C}}_s & \underline{\underline{A}}_g & 0 & \underline{\underline{B}}_g\underline{\underline{D}}_s & \underline{\underline{B}}_g \\ \hline 0 & \underline{\underline{D}}_g\underline{\underline{C}}_s & \underline{\underline{C}}_g & 0 & \underline{\underline{D}}_g\underline{\underline{D}}_s & \underline{\underline{D}}_g \\ \underline{\underline{C}}_t & -\underline{\underline{D}}_g\underline{\underline{C}}_s & -\underline{\underline{C}}_g & \underline{\underline{D}}_t & -\underline{\underline{D}}_g\underline{\underline{D}}_s & -\underline{\underline{D}}_g \end{array}\right] \tag{13}$$

With the system in- and output $\underline{\underline{P}}_{wu}$ is linked as follows.

$$\begin{bmatrix} \underline{z} \\ \underline{e} \end{bmatrix} = \underline{\underline{P}}_{wu} \begin{bmatrix} \underline{w}_r \\ \underline{w}_d \\ \underline{e} \end{bmatrix} \tag{14}$$

The dimensions of the individual systems and the complete system $\underline{\underline{P}}_{wu}$ can be found in Table I. The internal dimensions of the state-space model in (13) are represented in Table II. Such a weighting scheme is built up for each operating point p.

TABLE II
DIMENSIONS OF WEIGHTING SCHEME $\underline{\underline{P}}_{wu,p}$ IN (13)

	n_{nt}	n_{ns}	n_{ng}	n_y	n_u	n_u
n_{nt}						
n_{ns}						
n_{ng}						
n_y						
n_y						

Here the index was left out due to lack of space. The controller synthesis is carried out by the SLICOT function `SB10DD` for each operating point after delivery of the system $\underline{\underline{P}}_{wu,p}$ and a γ value. Beginning with a γ of 100 this is decreased in up to five iteration steps during successful synthesis.

The p SISO controllers, which are currently used for FIVE-BAR, have the order $n_{ng}+n_{ns}+n_{nt}$, which corresponds to the one of $\underline{\underline{P}}_{wu}$. The order of the plant is always reduced to 14 and the two weighting functions have in each case the order one, which corresponds to a controller order of 16.

The storage of the controllers at run-time takes place in an own state-space model class. For permanent storage on hard disk an own file data base is used.

F. Results

The integrated controller synthesis, presented in this article, is implemented and executable on the QNX computer. In many practical tests the operability was proven.

The following diagrams are results of a system identification and a controller synthesis done with that system. The Fig. 13 shows the result of the system identification of the plant $\underline{\underline{G}}$ in form of a Bode diagram. The broken line shows the measured frequency response of the real plant, which was computed from the time signal under Matlab with `tfe`. The continuous line shows the frequency response of the system identified under QNX. The correlation in amplitude and phase is very good. The drift, which can be recognized in the phase response, is a result of the anti-aliasing filters adjusted to a cut-off frequency of 100 Hz. A crucial advantage to the former procedure, which measured the plants characteristic with a FFT Analyzer, is that these filters are identified directly by identifying the plant. Former, the filters were added before the controller synthesis in Matlab, in order to model the phase response correctly.

The controller designed under QNX is exported to Matlab for analysis. With the state-space model of the plant the disturbance rejection $\underline{\underline{S}}\,\underline{\underline{G}}$ could be computed. Together with the open loop system $\underline{\underline{G}}$ and the inverse weighting function $\underline{\underline{W}}_{sg}^{-1}$, used in the synthesis, its singular values are represented in Fig. 14. In this design nearly only the first eigenfrequency is suppressed. It can be recognized that $\underline{\underline{W}}_{sg}^{-1}$ serves as an upper bound of $\underline{\underline{S}}\,\underline{\underline{G}}$. Except for the right boundary region, this is fulfilled everywhere.

A measure for the disturbance rejection is the sensitivity $\underline{\underline{S}}$. The sensitivity of the control loop is represented in Fig. 15. In this diagram it can be directly read off, that the maximum

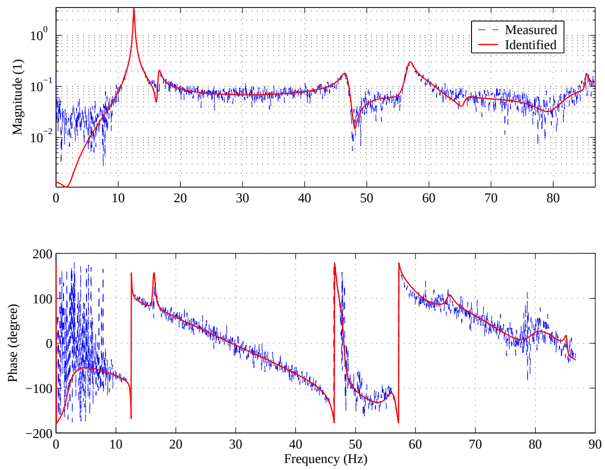

Fig. 13. Measured and Identified Systems FRF

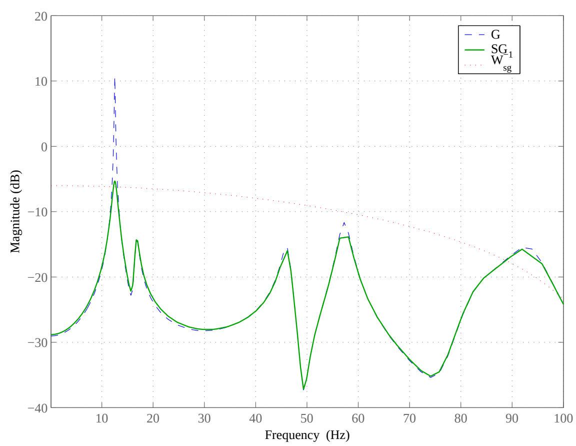

Fig. 14. Singular Values of $\underline{\underline{G}}$, $\underline{\underline{S}}\,\underline{\underline{G}}$ and $\underline{\underline{W}}_{sg}^{-1}$

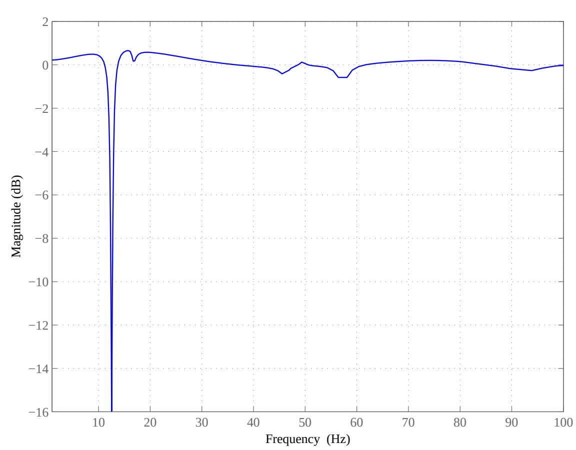

Fig. 15. Singular Values of Sensitivity $\underline{\underline{S}}$

suppression is -16dB and emerges at a frequency of 12 Hz.

The entire process of the measurement, signal processing, identification, controller synthesis and installation lasts only approx. 25 s on the QNX system, a PC with 2.4 GHz CPU and 512 MB RAM. The measurement already takes 19 s. The identification, controller synthesis and installation are at present still called by hand over the command line and need the remaining 6 s.

IV. Conclusion

In this article the method of Robust-Gain-Scheduling for robust $\mathcal{H}_\infty$ control of an adaptive system was presented. In order to improve the performance, the knowledge of the position of the effector was used and the workspace was divided according to a Voronoi diagram. The very time-consuming, former procedure for controller synthesis could be replaced by a newer and faster one. By the employment of the SLICOT library it is now possible to run the entire synthesis process on the realtime computer and thus to shorten its execution time to 25 s at present. With the help of this procedure one can react fast and without use of additional hardware to the sensitivity of the system to be controlled, e.g. after disassembly and assembling. Regarding industrial applications it is very suitable for practical use of structural control.

Future work will make the procedure more robust and more automated. The parameter setting of the weighting functions and a more exact analysis of the robustness of the control loop are two of these upcoming topics.

Acknowledgment

This work was funded by the 'Deutsche Forschungsgemeinschaft' within the framework of the Collaborative Research Center 562 'Robotic Systems for Handling and Assembly'.

References

[1] "Sonderforschungsbereich 562 - robotersysteme für handhabung und montage," TU Braunschweig und Deutsches Zentrum für Luft- und Raumfahrt e.V., Braunschweig, Finanzierungsantrag, 2003.

[2] J. Steiner and N. Kohn, "Universal communication architecture for high-dynamic robot systems using qnx," in *Proc. of ICARCV*, Kunming, China, 2004.

[3] E. Breitbach, S. Algermissen, R. Keimer, M. Rose, and C. Stachera, "Adaptive tools in parallel robotics," in *Robotic Systems for Handling and Assembly, 2nd International Colloquium of the Collaborative Research Center 562*, ser. Fortschritte in der Robotik, P. Last, C. Budde, and F. M. Wahl, Eds., vol. 9. Braunschweig, Germany: Shaker Verlag, 10-11 May 2005, pp. 203–219.

[4] R. Krten, *Getting Started with QNX Neutrino 2: A Guide for Realtime Programmers*. PARSE Software Devices, 2001.

[5] R. Keimer, M. Rose, and S. Algermissen, "Parallelroboter mit adaptronischer schwingungsunterdrückung am beispiel der versuchsstruktur fünfgelenk," in *Adaptronic Congress*, Wolfsburg, April 2003.

[6] S. Algermissen, M. Rose, R. Keimer, and E. Breitbach, "High-speed parallel robots with integrated vibration-suppression for handling and assembly," in *11th Annual International Symposium on Smart Structures and Materials*. San Diego, Kalifornien, USA: SPIE, März 2004.

[7] S. Algermissen, M. Rose, and R. Keimer, "Angewandte robuste regelung zur schwingungsunterdrückung am parallelroboter mit adaptronischen komponenten," in *Adaptronic Congress*, Hildesheim, April 2004.

[8] P. Benner, V. Mehrmann, V. Sima, S. V. Huffel, and A. Varga, "Slicot - a subroutine library in systems and control theory," *Applied and Computational Control, Signals, and Circuits*, vol. 1, no. 10, pp. 499–539, 1999.

[9] Slicot sources. [Online]. Available: ftp://wgs.esat.kuleuven.ac.be

[10] Clapack sources. [Online]. Available: http://netlib.org/clapack

[11] f2c sources. [Online]. Available: http://netlib.org/f2c

[12] E. C. Ifeachor and B. W. Jervis, *Digital Signal Processing: A Practical Approach*, 2nd ed. Prentice Hall, 2001.

[13] W. Favoreel, V. Sima, S. V. Huffel, M. Verhaegen, and B. D. Moor, "Slicot working note 19986: Subspace model identification of linear systems in slicot," European Community BRITEEU-RAM III Thematic Networks Programme NICONET, Tech. Rep., 1998, anonymous ftp from wgs.esat.kuleuven.ac.be in the directory pub/WGS/REPORTS/SLWN19986.ps.Z.

[14] M. S. Tombs and I. Postlethwaite, "Truncated balanced realization of stable, non-minimal state-space systems," *International Journal of Control*, vol. 46, pp. 1319–1330, 1987.

[15] K. Zhou, J. Doyle, and K. Glover, *Robust and Optimal Control*. Prentice Hall, 1996.

[16] H. Unbehauen, *Regelungstechnik 2: Zustandsregelungen, digitale und nichtlineare Regelsysteme*. Vieweg, 1997.